Supplementary Information

A surface-attached Ru complex operating as rapid bistable molecular switch

George Tsekouras, Olof Johansson and Reiner Lomoth

Experimental

Electrode preparation

The Pt microdisc electrodes (Ø 100 μm) were polished with alumina (0.3 μm, Buehler), rinsed with deionised (DI) water and sonicated for 1 min in DI water. The electrodes were then electrochemically cleaned in degassed 0.5 M H_2SO_4 (Sigma-Aldrich, 99.999%) over 15 cyclic voltammetry (CV) scans between -0.21 V and 1.45 V vs. Ag/AgCl followed by two scans between -0.20 V and 1.35 V. For both sets of scans, the scan rate was 0.1 Vs^{-1} and scans started and ended within the capacitive region at 0.3 V (Figure S1). For the electrode later modified with the Ru complex a surface area of 7.4×10^{-4} cm^2 was determined from the charge under the PtO reduction peak at 0.50 V (3.1×10^{-7} C) and a value of 4.20×10^{-4} C cm^{-2} for reduction of the oxide monolayer. Comparison to the geometric area of 7.85×10^{-5} cm^2 indicates that the described treatment of the electrode results in a relatively high roughness factor of about 9.

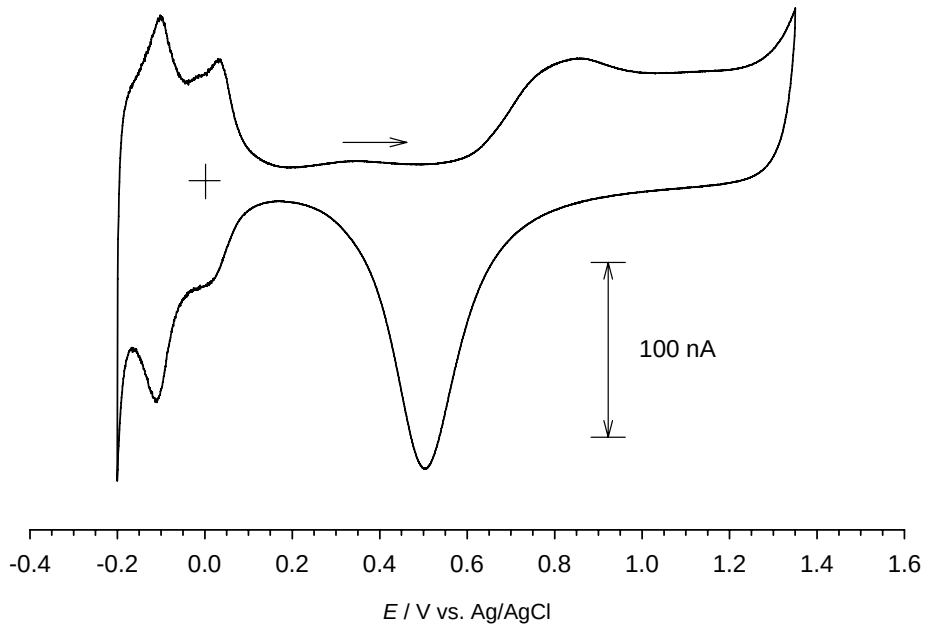

Figure S1. CV (scan 2) of a Pt microelectrode (Ø 100 μm) in degassed 0.5 M H_2SO_4 at a scan rate of 0.100 Vs^{-1}.

Electrodes were immersed overnight in 11-amino-1-undecanethiol solution (10 mM in EtOH, Dojindo) to yield an amine-terminated SAM. The modified electrodes were then placed overnight in a stirred solution (THF:CH_3CN, 5:1) of the carboxylate terminated ruthenium complex **1**[1] (0.1% w/v) with 4-(4,6-dimethoxy-1,3,5-triazin-2-yl)-4-methylmorpholinium chloride (DMTMM, 1% w/v, Fluka) as coupling agent.[2,3]

---

[1] Complex **1** was prepared as previously described. (G. Tsekouras, N. Minder, E. Figgemeier, O. Johansson and R. Lomoth, *J. Mater. Chem.*, **2008**, *18*, 5824 – 5829)

[2] M. Kunishima, C. Kawachi, J. Morita, K. Terao, F. Iwasaki and S. Tani, *Tetrahedron*, 1999, **55**, 13159-13170.

[3] Compared to *N*-(3-dimethylaminopropyl)-*N'*-ethylcarbodiimide (see e.g. R. M. Haddox and H. O. Finklea, *J. Phys. Chem. B*, **2004**, *108*, 1694-1700), DMTMM yields superior surface coverage results if the coupling reaction involves aromatic carboxylic acids. (M. Sjödin, unpublished results.)

In the final step of monolayer-modified electrode preparation, electrodes were placed for 3 hrs in a solution of 6-mercapto-1-hexanol (10 mM in EtOH, Sigma-Aldrich) in order to re-pack the electrode surface and thereby greatly minimise the background capacitive response during cyclic voltammetry (CV).

Eletrochemical measurements

All electrochemical measurements were performed in CH_3CN (Sigma-Aldrich, spectrophotometric grade) with 0.1 M $TBAPF_6$ (Fluka, puriss., electrochemical grade) as supporting electrolyte using the Autolab PGSTAT302 potentiostat equipped with the SCANGEN analog sweep generator and ADC750 fast sampling A/D converter (750 kHz) modules and controlled with the GPES 4.9 software (ECO Chemie B.V., Utrecht, The Netherlands). CVs were recorded in a 3-electrode cell consisting of a Pt disk (Ø 100 μm) working electrode, a glassy carbon rod auxiliary electrode and a non-aqueous Ag/Ag^+ reference electrode (CH instruments Inc., Austin, Texas, 0.01 M $AgNO_3$ and 0.1 M $TBAPF_6$ in CH_3CN). Both reference and auxiliary electrode used a salt bridge with 0.1 M $TBAPF_6$ in CH_3CN. All potentials were reported against the ferrocene/ferrocenium (Fc/Fc^+) redox couple.

The voltammograms were corrected for most of the capacitive charging currents by subtracting the background response of the underlying amine-terminated SAM (Figures S2-S4). The latter was obtained from CVs of thiol-modified electrodes without the Ru complex attached. To account for minor differences in capacitance between the Ru modified electrode and the electrode used for the background measurements, a scaling factor of about 1.05 to 1.1 was applied to the background to adjust it to the purely capacitive parts of the CVs. For the background corrected CVs, peak heights and areas were determined on top of linear baselines (Figure 1 and S4) that warrant equal total charges under oxidation and reduction peaks, respectively.[4]

Figure S5 shows the scan rate dependence of the peak potentials that are controlled by the isomerization kinetics at low scan rates and by electron transfer kinetics at high scan rates where kinetic control over the peak potentials can be neglected and formal potentials were determined from the averages of peak potentials $E^{o\prime}(N_6) = ½(E_{pA}+E_{pA'})$ and $E^{o\prime}(N_5O) = ½(E_{pB}+E_{pB'})$. Figure S6 shows the peak widths for different scan rates.

[4] The incomplete subtraction of charging current on the reverse scans might indicate increased double layer capacity due to the influx of counterions upon oxidation of the Ru complexes.

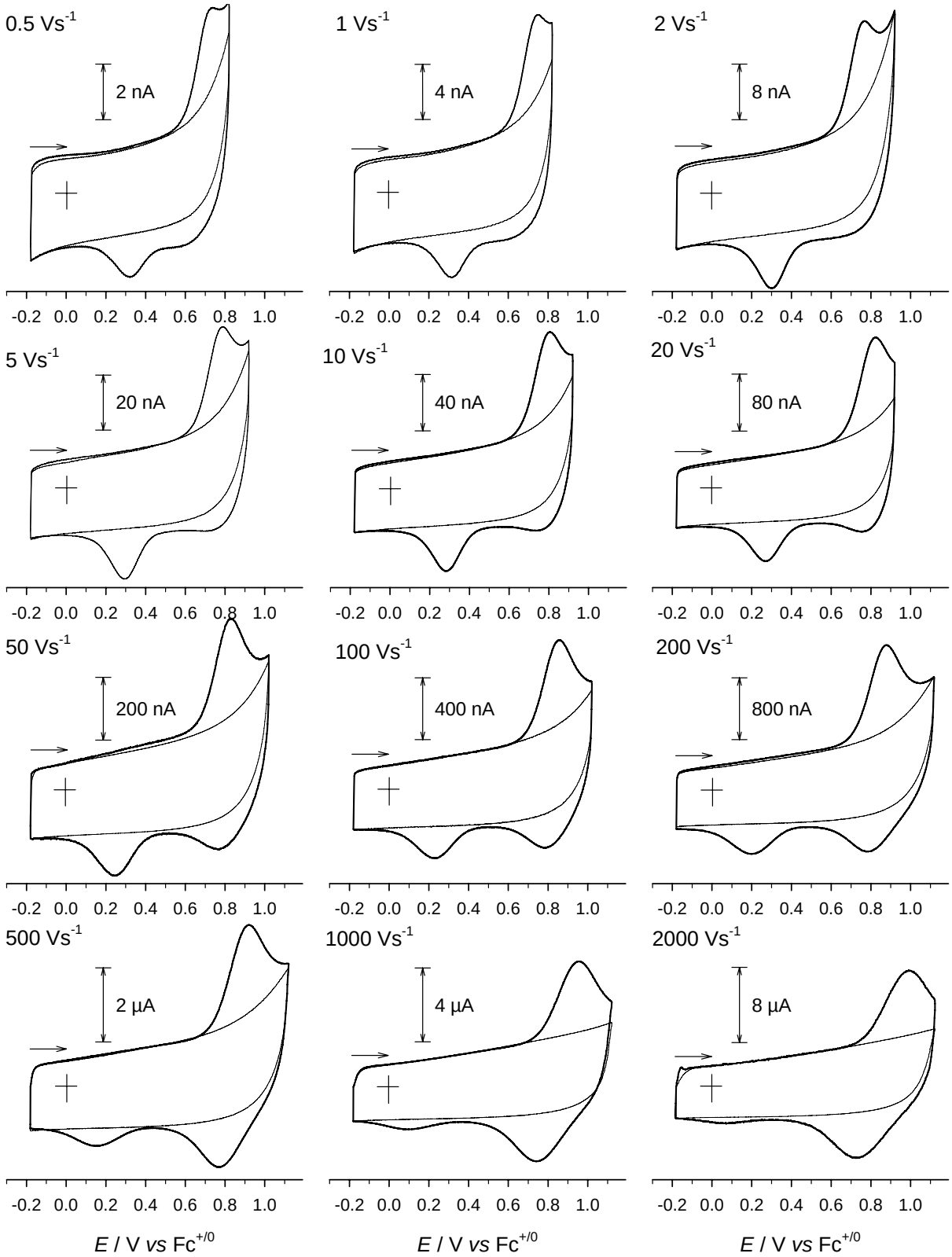

Figure S2. Voltammograms (scan 1) of complex **1** immobilized on Pt microelectrode (**—**) and scaled background response of the underlying amine-terminated SAM (—) recorded in CH_3CN with 0.1 M $TBAPF_6$ at the indicated scan rates.

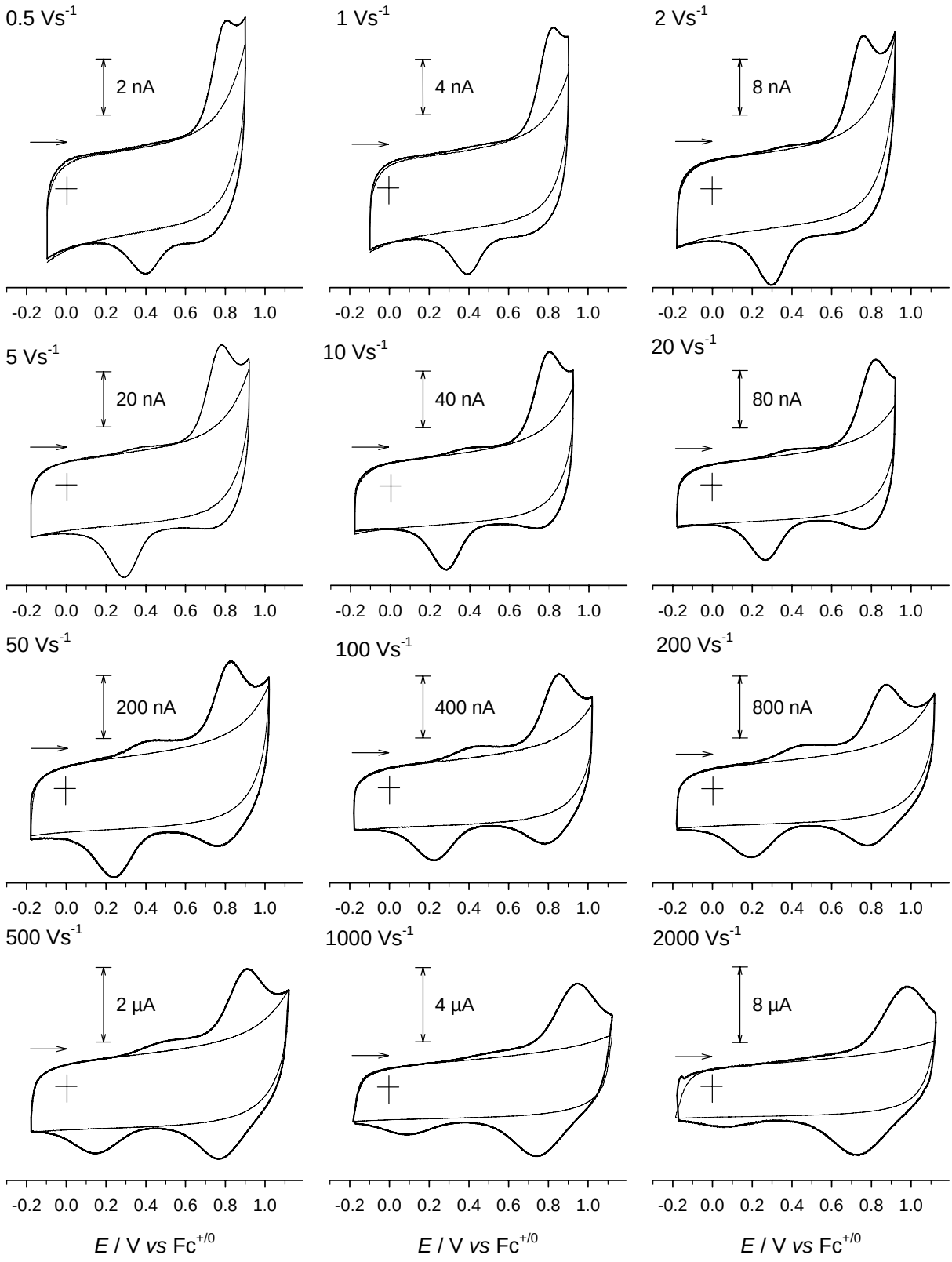

Figure S3. Voltammograms (scan 2) of complex **1** immobilized on Pt microelectrode (**—**) and scaled background response of the underlying amine-terminated SAM (—) recorded in CH_3CN with 0.1 M $TBAPF_6$ at the indicated scan rates.

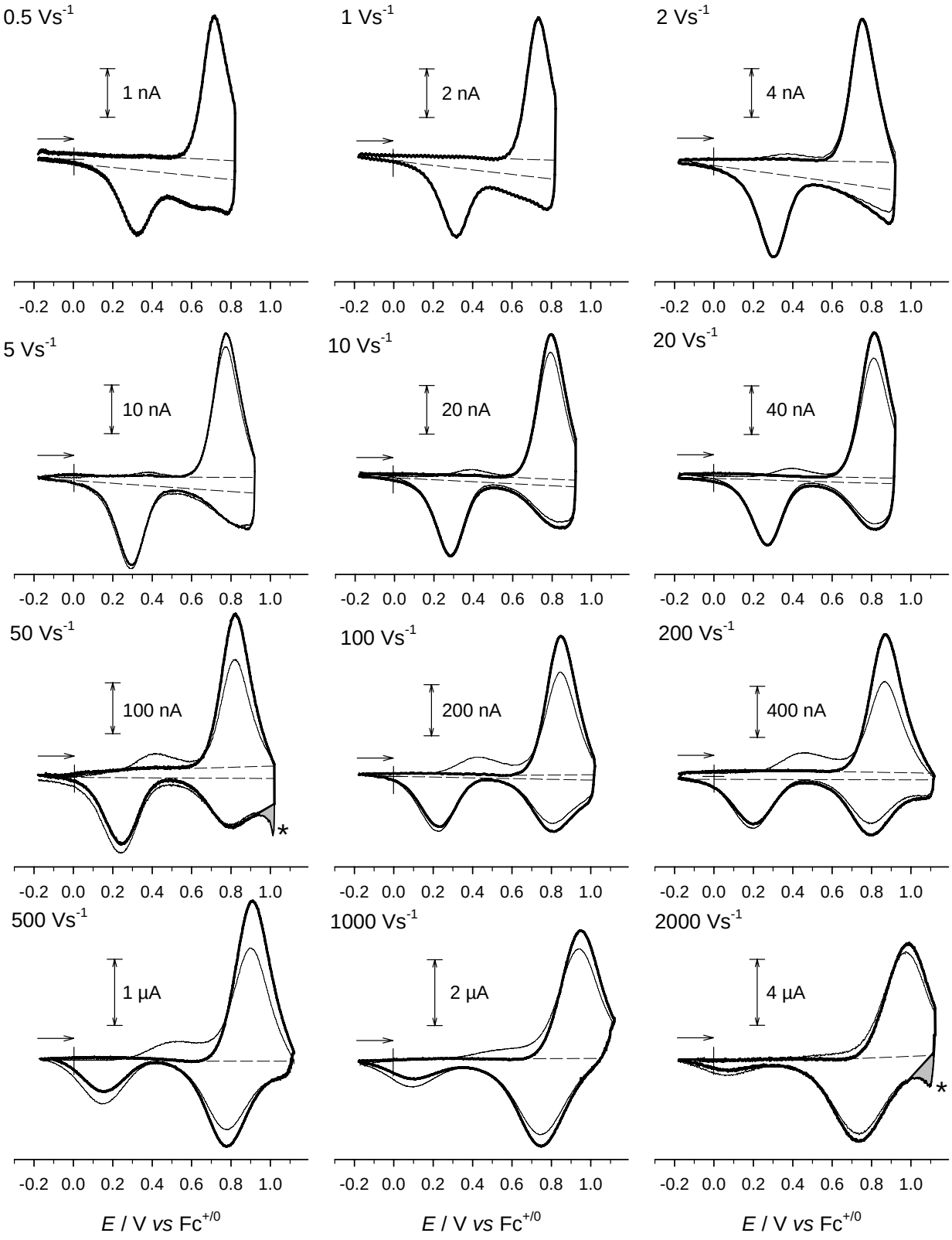

Figure S4. Voltammograms of complex **1** immobilized on Pt microelectrode (background corrected for capacitive response of the underlying amine-terminated SAM). Scan 1 (**—**) and scan 2 (—) recorded in CH_3CN with 0.1 M $TBAPF_6$ at the indicated scan rates. Peak heights and areas were determined in respect to the indicated baselines (---). (*) Background subtraction artifacts due to lower potentiostat bandwith for background measurement. Shaded area not included in peak area.

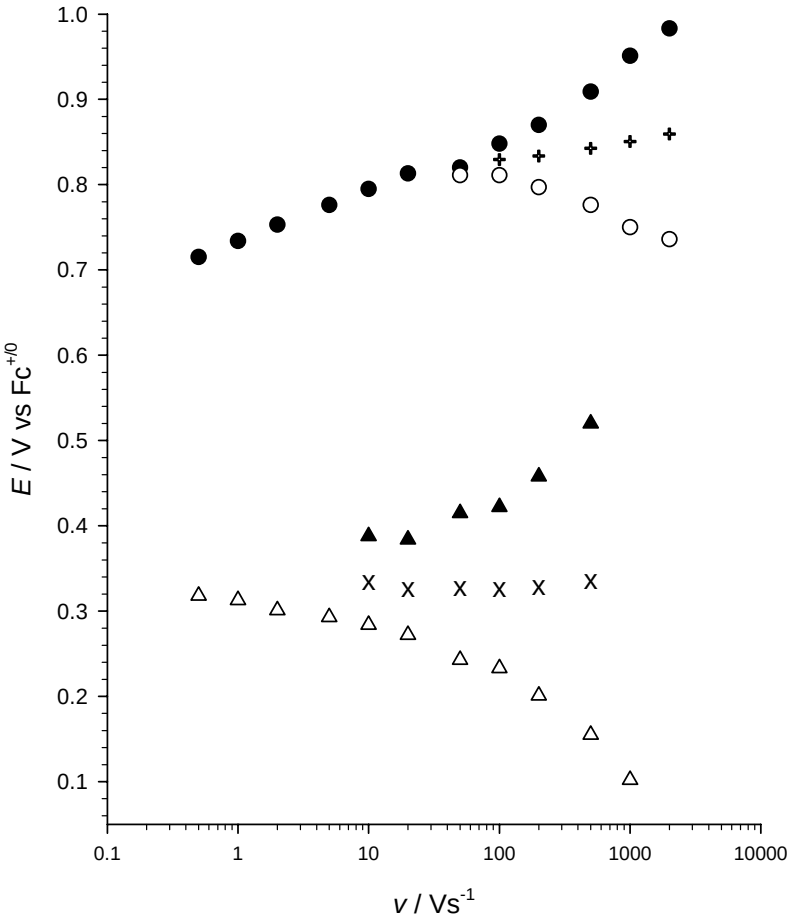

Figure S5. Peak potentials as function of scan rate for peak A(●), A'(○), B(▲) , and B'(△) and average potentials ½(E_{pA}+$E_{pA'}$) (+) and ½(E_{pB}+$E_{pB'}$) (×).

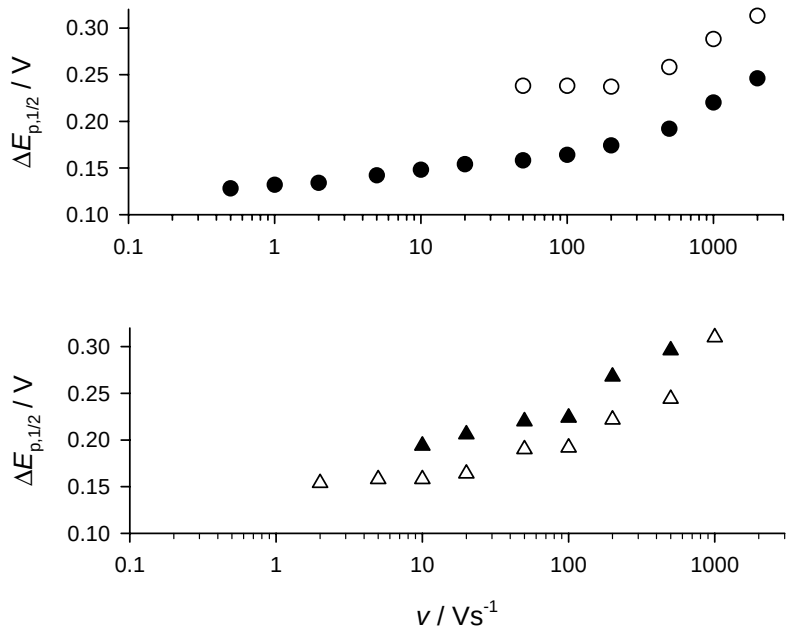

Figure S6. Peak widths (fwhm) as function of scan rate for peak A(●), A'(○), B(▲) , and B'(△).